# The Effect of Gamma Irradiation on Electrical Characteristics of Au/Polyvinyl Alcohol (Co, Zn-Doped)/n-Si Schottky Barrier Diodes

**İ. Taşçıoğlu,[1] H. Uslu,[1] Ş. Altındal,[1] P. Durmuş,[1] İ. Dökme,[2] T. Tunç[3]**

[1] *Department of Physics, Faculty of Science and Arts, Gazi University, Ankara 06500, Turkey*
[2] *Science Education Department, Faculty of Education, Gazi University, Ankara, Turkey*
[3] *Science Education Department, Faculty of Education, Aksaray University, Aksaray, Turkey*

Received 21 January 2010; accepted 13 March 2010
DOI 10.1002/app.32450

**ABSTRACT:** To show the effect of gamma radiation, Au/Polyvinyl Alcohol (Co, Zn-doped)/n-Si Schottky barrier diodes (SBDs) were exposed to $^{60}$Co γ-ray source at room temperature. These structures were investigated by using current-voltage (*I-V*), capacitance-voltage (*C-V*), and conductance-voltage (*G*/ω-*V*) measurement methods before and after irradiation. The *C-V* and *G*/ω-*V* measurements were carried out at 1 MHz. The density of interface states ($N_{ss}$) as a function of $E_c$-$E_{ss}$ was obtained from the forward bias *I-V* data by taking into account the bias dependence effective barrier height ($\Phi_e$) and series resistance ($R_s$) of device at room temperature. Experimental results show that the values of ideality factor (*n*), $R_s$, and $N_{ss}$ increased after gamma irradiation. It was found to degrade the reverse leakage current with radiation whereas its effect on the forward *I-V* characteristics was negligible. The results show that main effect of the radiation is the generation of $N_{ss}$ with energy level within the forbidden band gap of Si between polymer and semiconductor. In addition, the values of $R_s$ were determined from Cheung's method, and it was seen that these values increased with radiation effect. As seen *I-V* and *C-V* characteristics, the main electrical parameters such as ideality factor (*n*), $R_s$, $N_{ss}$ were strongly influenced with the presence of radiation. © 2010 Wiley Periodicals, Inc. J Appl Polym Sci 118: 596–603, 2010

**Key words:** Au/polyvinyl alcohol (Co, Zn-doped)/n-Si schottky barrier diodes (SBDs); radiation effects; interface states; series resistance

## INTRODUCTION

The inorganic–organic electronic devices such as metal-polymer-semiconductor (MPS) type Schottky barrier diodes (SBDs), light-emitting diodes, and solar cells have potential advantages compared to traditional inorganic these devices because of their lower production costs, light weight, and processibility on flexible substrates.[1–3] The behaviors of electrical characteristics of MPS structures are similar to metal/insulator/semiconductor (MIS) type SBDs. These devices are considered by many in the field to shape the next generation of cheap and disposable electronic inventions.[4–7] The electrical properties of metal-semiconductor (MS) SBDs can be modified by metal doped (such as Co, Ni, Zn) polymer materials, when these organic interfacial layers are inserted between the inorganic semiconductor and metal. Polyvinyl alcohol (PVA) is the most interesting material among the other polymers in view of its large scale applications. Special properties of PVA arise from the role of OH groups and hydrogen bonding. PVA is normally a poor electrical conductor; it becomes conductive upon doping with some dopants. Over recent years, PVA, polyaniline, poly (alkylthiophene) polypyrrole, polyophene, poly (3-hexylthiophene) have been the focus attention because of their rich variety of applications such as Schottky barrier diodes and solar cells.[3–9] These devices based on organic materials are influenced not only by the structure and nature of a dopant material but also by the doping concentration and procedure.[10]

Studying the effect of ionizing radiation has been of interest, especially the physical properties of semiconductor devices. In satellite communication, the semiconductor devices used have been exposed to rays. This causes radiation ionization of the semiconductor devices, which may destroy the characteristics of these devices.[11] Therefore, the radiation dependent characteristics of physical parameters such as ideality factor (*n*), barrier height ($\Phi_b$), series resistance ($R_s$), and interface states ($N_{ss}$) have become a subject of very intensive research and reported in the literature for more than 3 decades.[12–15]

$^{60}$Co (γ-rays) has become one of the most common processes producing modifications in electrical, chemical, and morphological properties of SBDs.[10,16,17] The electrical characteristics of these devices especially depend on the formation of an interfacial insulator/

---

*Correspondence to:* İ. Taşçıoğlu (ilketascioglu@gazi.edu.tr).

Journal of Applied Polymer Science, Vol. 118, 596–603 (2010)

polymer layer, barrier height (BH), interface properties at metal/semiconductor (M/S) interface, series resistance of device ($R_s$), and surface states at polymer/semiconductor interface.[18–22]

In general, the capacitance ($C$) value shows an increase with an increase in the bias voltage. However, in recent years, some investigators have reported[22–26] an anomalous peak in the forward bias $C$-$V$ characteristics. Among them, Chattopadhyay and Raychaudhuri[23] show that the magnitude peak value of $C$ and its position depend on various parameters such as $N_{ss}$, doping concentration ($N_A$ or $N_D$), $R_s$, and thickness of insulator layer. The origin of such peak in $C$-$V$ plots has been ascribed to interface states by Ho et al.[26] Recently, the electrical properties of these devices have been found to change significantly when these devices are exposed to high-level particles (gamma, electrons, protons, ions).[27–31] Winokur et al.[29,30] and Ma[31] were the first to make a systematic observation of the after irradiation behavior of $N_{ss}$ in MIS devices. There are two important effects of radiation: a transient effect due to the electron-hole pair generation and a permanent effect to the bombardment of devices with radiation which causes changes in the crystal lattice. Radiation generates these electron-hole pairs in the insulator/polymer that subsequently interact with trapping sites with the insulating film. While the radiation generated electrons either recombine with the holes or move out of insulator, the radiation generated holes may diffuse in the insulator, but are less mobile than the electrons; many stationary hole traps are also present.

In this work, Au/PVA (Co, Zn-doped)/n-Si SBD$_s$ were exposed to dose of 22 kGy to see the effect of $^{60}$Co ($\gamma$-rays) on the main electrical parameters of Au/PVA (Co, Zn-doped)/n-Si SBD$_s$ such as ideality factor ($n$), zero-bias barrier height ($\Phi_{bo}$), series resistance ($R_s$) of device, doping carrier concentration ($N_D$), and density of interface states ($N_{ss}$). These parameters, before and after irradiation, have been investigated by using the forward and reverse bias $I$-$V$, $C$-$V$, and $G/\omega$-$V$ measurement methods at room temperature. The major purpose of this work is to investigate damage effect centers induced by $\gamma$-ray irradiation and study their effect on performance of these structures.

## EXPERIMENTAL DETAIL

The Au/PVA (Co, Zn-doped)/n-Si SB devices were fabricated on the 2 inch (5.08 cm) diameter flot zone (111) n-type (phosphor doped) single crystal Si wafer having thickness of 350 μm with ≅0.7 Ωcm. Si wafer first was cleaned in a mix of a peroxide-ammoniac solution and then in $H_2O + HCl$ solution for 10 min. After it was thoroughly rinsed in deionised water resistivity of 18 MΩcm using an ultrasonic bath for 15 min, immediately high purity Au metal (99.999 %) with a thickness of about 2000 Å was thermally evaporated onto the whole back side of Si wafer in a pressure about $10^{-6}$ Torr in high vacuum system. To perform a low resistivity ohmic back contact, Si wafer was sintered at 450°C for 5 min in $N_2$ atmosphere.[7]

The PVA film was fabricated on n-type Si by electrospinning technique. A simple illustration of the electrospinning system is given in Figure 1. Cobalt acetate of 0.5 g and zinc acetate of 0.25 g was mixed with 1 g of PVA, molecular weight = 72,000 and 9 mL of deionised water. After vigorous stirring for 2 h at 50°C, a viscous solution of PVA/(Co, Zn-dopped) acetates was obtained. Using a peristaltic syringe pump, the precursor solution was delivered to a metal needle syringe (10 mL) with an inner diameter of 0.9 mm at a constant flow rate of 0.02 mL/h. The needle was connected to a high voltage power supply and positioned vertically on a clamp. A piece of flat aluminum foil was placed 15 cm below the tip of the needle to collect the nanofibers. Si wafer was placed on the aluminum foil. Upon applying a high voltage of 20 kV on the needle, a fluid jet was ejected from the tip. The solvent evaporated and a charged fiber was deposited onto the Si wafer as a nonwoven mat. After spinning process, circular dots of 1 mm in diameter and 1500 Å thick high purity Au rectifying contacts were deposited on the PVA surface of the wafer through a metal shadow mask in liquid nitrogen traped oil-free ultra high vacuum system in the pressure of about $10^{-7}$ Torr.

Before fabricated rectifying contact the PVA doped with different ratio of Cobalt and Zinc composite electrospun fibers film on Si produced were examined using SEM micrographs. Fiber formation and morphology of the electrospun Co-Zn/PVA fibers were determined using a Scanning Electron Microscope (SEM) Quanto 400 FEI MK-2 of the PHB film was taken digitally at 20 kV. The diameter of nonwoven fibers was analyzed using ImageJ (Image Prossing and Analyzing in Java) digital image analysis program.

The $I$-$V$, $C$-$V$, and $G/\omega$-$V$ measurements were performed before and after $^{60}$Co $\gamma$-ray source irradiation with the dose rate of 1.12 kGy/h at room temperature. The $I$-$V$ measurements were carried out using a Keithley 220 programmable constant-current source and a Keithley 614 electrometer. The $C$-$V$ and $G/\omega$-$V$ measurements were carried out using an HP 4192A LF impedance analyzer (5 Hz–13 MHz), and small sinusoidal test signal of 40 mV$_{p\text{-}p}$ from the external pulse generator was applied to the sample to meet the requirement. All measurements were carried out with the help of a microcomputer through an IEEE-488 ac/dc converter card.

## RESULTS AND DISCUSSION

### Effects of gamma irradiation on the *I-V* characteristics

To quantitatively analyze the Au/PVA (Co, Zn-doped)/n-Si Schottky barrier diodes (SBDs) characteristics, we

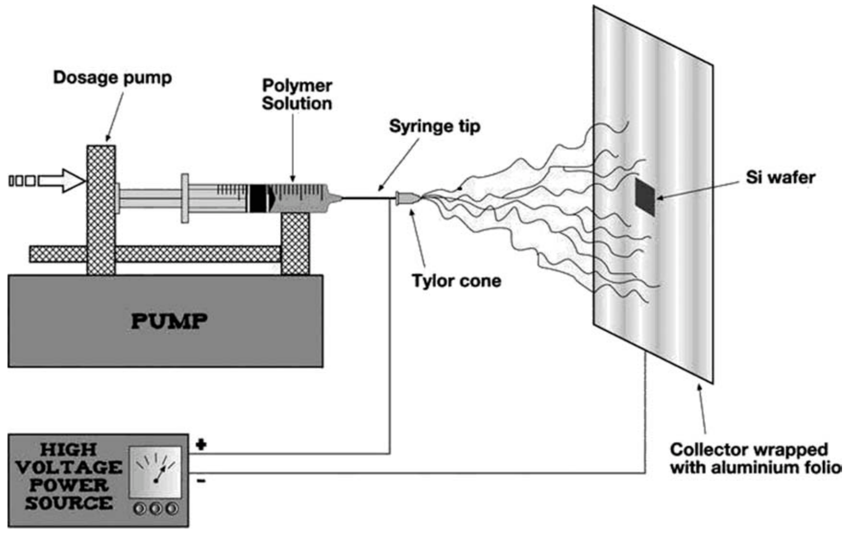

**Figure 1** Schematic representation of the electrospinning process.

assume the standard thermionic emission (TE) theory as follows[18]

$$I = I_o \exp\left(\frac{qV_d}{nkT}\right)\left[1 - \exp\left(\frac{-qV_d}{kT}\right)\right] \quad (1)$$

$$I_o = A\,A^{*}T^{2}\ \exp\left(-\frac{q\Phi_{\mathrm{bo}}}{kT}\right) \quad (2)$$

where $V_d$ is the voltage drop across the diode, $q$ is the electronic charge, $A$ is the rectifier contact area, $k$ is the Boltzmann constant, $T$ is the absolute temperature in K, $A^*$ is the effective Richardson's constant of 120 A cm$^{-2}$ K$^{-2}$ for n-type Si, $\Phi_{\mathrm{bo}}$ is the zero bias barrier height (BH), $n$ is the ideality factor, and $I_o$ is the reverse saturation current. The ideality factor is a measure of the conformity of the diode current to be pure TE and it is calculated from the slope of the linear region of the forward bias Ln$I$ vs. $V$ plot and it can be written from eq. (1) as

$$\diamond\, n = \frac{q}{kT}\frac{dV_d}{d\mathrm{Ln}(I)} \quad (3a)$$

where $dV_d/d\mathrm{Ln}(I)$ is the slope of linear region of Ln$I$ vs. $V$ plots. Also, voltage dependent ideality factor $n(V)$ can be written from eq. (1) as[20]

$$n(V) = \frac{qV_d}{kT\mathrm{Ln}(I/I_0)} \quad (3b)$$

The zero bias barrier height ($\Phi_{\mathrm{bo}}$) is calculated from the extrapolated $I_o$ at zero bias and is given by

$$\Phi_{\mathrm{bo}} = \frac{kT}{q}\mathrm{Ln}\left(\frac{AA^{**}T^{2}}{I_o}\right) \quad (4)$$

From a linear fit of the Ln$I$ vs. $V$ plots in Figure 2, the experimental values of $n$ and $\Phi_{\mathrm{bo}}$ were calculated by the slopes and intercepts of linear fits. The $n$ and $\Phi_{\mathrm{bo}}$ values were found as 2.12 and 0.69 eV (before radiation) and 2.68 and 0.66 eV (at 22 kGy), respectively. High values of $n$ can be attributed to the presence of the interfacial polymer layer, barrier inhomogeneity and the applied bias voltage dependence of the barrier height.[18–20,32,33] Such behaviour of $n$ can be attributed to an increase in radiation induced defects ($N_{\mathrm{ss}}$) in the crystal lattice and a stretch in depletion layer ($W_D$) as indicated by the incoming relation[20]

$$n = 1 + \frac{\delta}{\varepsilon_i}\left(\frac{\varepsilon_s}{W_D} + qN_{\mathrm{ss}}\right) \quad (5)$$

where $W_D$ is the space charge width, $\varepsilon_i$ and $\varepsilon_s$ are the permittivity of semiconductor and interfacial layer, respectively.

The value of leakage current after γ-irradiation is almost one order of magnitude higher than before irradiation. This increase in the leakage current is undesired situation in view of the performance of diode. Also, there is almost saturation behaviour in the reverse bias current. In contrary to the $I_o$ and $n$, the value of BH is almost unchanged with γ-irradiation. As shown in Figure 2, the current values in the forward bias region are almost unchanged with γ-irradiation.

According to Ref. 32, the forward bias $I$-$V$ characteristics due to the thermionic emission (TE) theory of a SBD with the series resistance ($R_s$), eq. (1), can be rewritten as

$$I = I_o \exp\left(\frac{q(V - IR_s)}{nkT}\right)\left[1 - \exp\left(\frac{-q(V - IR_s)}{kT}\right)\right] \quad (6)$$

where the term of $IRs$ is the voltage drop across the $R_s$. The $R_s$ is significant in the downward curvature

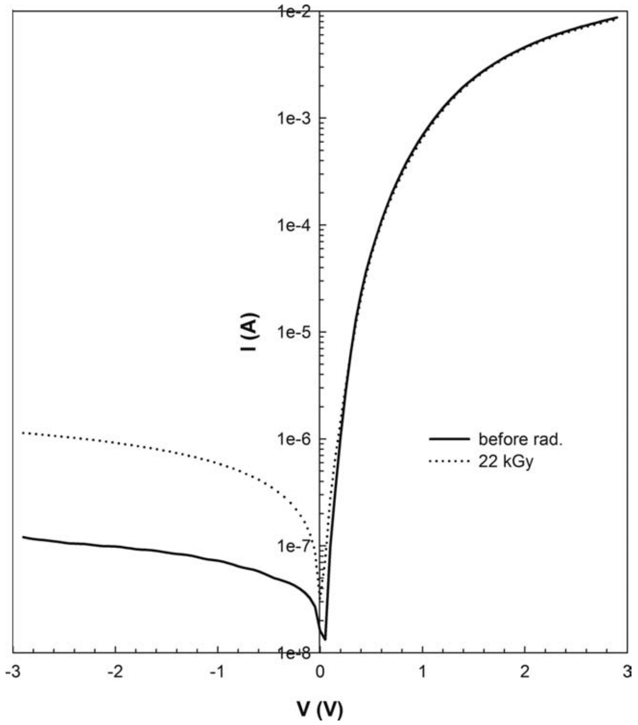

**Figure 2** Forward and reverse bias *I-V* characteristics of Au/PVA (Co, Zn-doped)/n-Si Schottky diodes before and after radiation.

of the forward bias *I-V* characteristics, but $N_{ss}$ is significant in both linear and nonlinear regions of the *I-V* characteristics.

The effect of series resistance ($R_s$) on Ln*I* vs. *V* plots can be analyzed by Cheung's method defined by the following relation,[34]

$$\frac{dV}{d\mathrm{Ln}I} = n\frac{kT}{q} + R_s I \qquad (7a)$$

$$H(I) = V - n\frac{kT}{q}\mathrm{Ln}\left(\frac{I_o}{AA^*T^2}\right) = n\Phi_b + R_s I \qquad (7b)$$

where $\Phi_b$ is the BH and $q$ is the electronic charge.

Figure 3(a,b) show the experimental *dV/d*Ln*(I)* vs. *I* and *H(I)* vs. *I* plots before and after radiation for PVA (Co, Zn-doped)/n-Si SBD, respectively. Thus, the slope and y-axis intercept of *dV/dLnI* vs. *I* plots according to eq. (7a) will give $R_s$ and $n(kT/q)$ for PVA (Co, Zn-doped)/n-Si SBDs, respectively. A plot of *H(I)* vs. *I* according to eq. (7b) will also give a straight line with y-axis intercept equal to $n\Phi_b$. The series resistances ($R_s$) were found to be 252.44 Ω before irradiation and 318.19 Ω after irradiation from eq. (7a) and also were found to 216.29 Ω before irradiation and 233.28 Ω after irradiation from eq. (7b), respectively. As seen Figure 3(a,b), the values of $R_s$ obtained from *dV/d(*ln*I)-I* and *H(I)-I* plots are closed with each other and increase after radiation. Such behavior of $R_s$ may be explained as being due to changes in the effective dopant density due to carrier removal by the defects produced.[35]

When a forward bias *V* is applied across the diode, it will be shared by interfacial layer ($V_i$), the depletion layer ($V_s$), and series resistance combination of the diode $R_s$, and thus *V* can be given as

$$V = V_s + V_i + IR_s \qquad (8)$$

When the interfacial layer is sufficiently thick and the transmission probability is very small, the effective barrier height ($\Phi_e$) is assumed to be applied bias-dependent due to the presence of an interfacial insulator layer and $N_{ss}$ located at M/S interface and is given by[20,36–38]

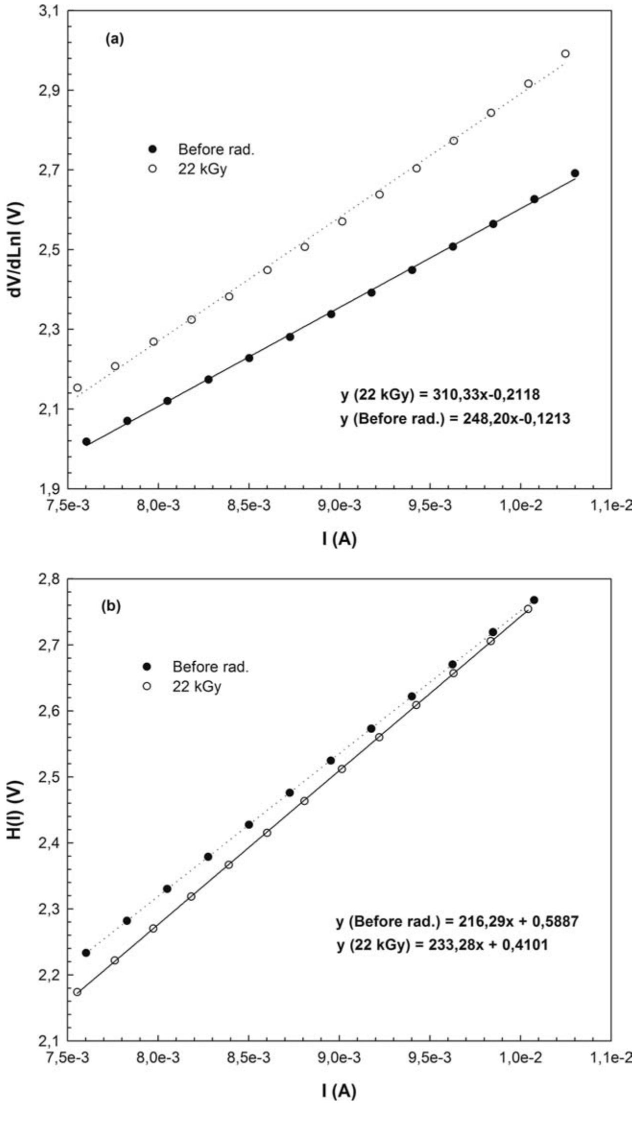

**Figure 3** The characteristics of Au/PVA (Co, Zn-doped)/n-Si Schottky diodes before and after radiation (a) *dV/d*ln*(I)* vs. *I* and (b) *H (I)* vs. *I*.

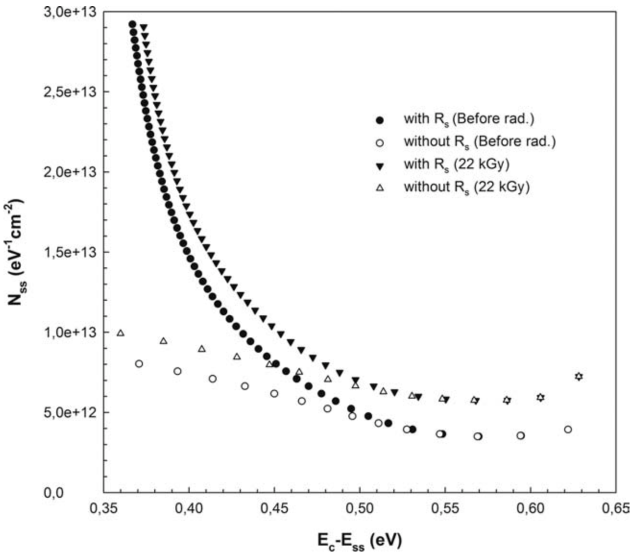

**Figure 4** The $N_{ss}$ profiles of Au/PVA (Co, Zn-doped)/n-Si Schottky diodes obtained from the forward bias *I-V* characteristics before and after irradiation.

$$\Phi_e = \Phi_{bo} + \alpha(V - IR_s) = \Phi_{bo} + \left(1 - \frac{1}{n(V)}\right)(V - IR_s) \tag{9}$$

where α is the voltage coefficient of the $\Phi_e$. During the elaboration of semiconductor devices of the MS and MIS types, defects appear which lead to electronic states with energies located in the forbidden band, the band gap. These states are known as interface states and alter the functioning of such devices. The interface states, organic interfacial layer (polymer) at metal/semiconductor interface play an important role in the determination of the main characteristics parameters of the devices. Interface states originate from defects such as dangling bounds at the insulator/substrate interface with energy states in the Si forbidden band gap and are dependent on the chemical composition of the interface, the interruption of the periodic lattice structure at the surface, surface preparation conditions, formation of insulator or polymer layer at M/S interface, and impurity concentration of semiconductor.[18,32] It is evaluated that interface properties of Au/n-Si structure are changed especially depending on the organic layer (polymer) inserted into metal and semiconductor, and this organic layer cause a significant modification of interface states.[15]

For MIS type SBD with $N_{ss}$ which is in equilibrium with semiconductor, the expression for $N_{ss}$ deduced by Card and Rhoderick[20] is reduced to[20,36–38]

$$N_{ss}(V) = \frac{1}{q}\left[\frac{\varepsilon_i}{\delta}(n(V) - 1) - \frac{\varepsilon_s}{W_D}\right] \tag{10}$$

where $\varepsilon_I$ (= 8 $\varepsilon_o$ ) and $\varepsilon_s$ (= 11.8 $\varepsilon_o$) are the permittivities of the interfacial layer and the semiconductor, respectively, $\varepsilon_o$ is the permittivity of free space ($\varepsilon_o$= 8,85 × $10^{-14}$ F/cm). δ is the thickness of the interfacial layer, and $W_D$ is the width of space charge region. Furthermore, in n-type semiconductors, the energy of interface states $E_{ss}$ with respect to the bottom of the conduction band at the surface of the semiconductor is given by[37]

$$E_c - E_{ss} = q[\Phi_e - (V - IR_s)] \tag{11}$$

The energy distribution profiles of $N_{ss}$ before and after irradiation given in Figure 4 were extracted from the forward bias *I-V* characteristics taking into account with and without $R_s$ obtained from Cheung's methods. As can be seen in the Figure 4, the exponential growth of the $N_{ss}$ from midgap of Si toward the bottom of the conductance band both before and after irradiation is very apparent. The values of $N_{ss}$ increase after irradiation due to radiation induced interface states. It is clear that the values of $N_{ss}$ obtained taking into account the $R_s$ are about one order lower than those obtained without considering the $R_s$, particularly near the conduction band. Therefore, the effect of $R_s$ must be taken into account in calculations of main electrical parameters such as $n$, $\Phi_b$, and $N_{ss}$.

### Effects of gamma irradiation on the *C-V* and *G/ω-V* characteristics

The *C-V* and *G/ω-V* characteristics of the unirradiated and irradiated Au/PVA (Co, Zn-doped)/n-Si SBD were measured at 1MHz and are given in Figure 5(a,b), respectively. As shown in Figure 5, the *C-V* and *G/ω-V* curves show a significant difference after irradiation especially in the depletion regions. It is clear that the *C-V* plot shows a peak in the accumulation region due to effect of $R_s$. Such behavior of *C-V* and *G/ω-V* plots show that the $N_{ss}$ is significant in the depletion and weak accumulation regions, but the $R_s$ is significant only in the strong accumulation region.

The real values of $R_s$ given in Figure 6 were calculated from the *C-V* and *G/ω-V* measurements at 1 MHz by using following equation[39]

$$R_s = \frac{G_{ma}}{G_{ma}^2 + \omega^2 C_{ma}^2} \tag{12}$$

Here, $C_m$ and $G_m/\omega$ are values of measured capacitance and conductance. These very significant values demanded the special attention be given to effects of the $R_s$ in the application of the admittance-based *C-V* and *G/ω-V* measured methods. As seen in Figure 6, the $R_s$ gives a peak in the −0,55 V and

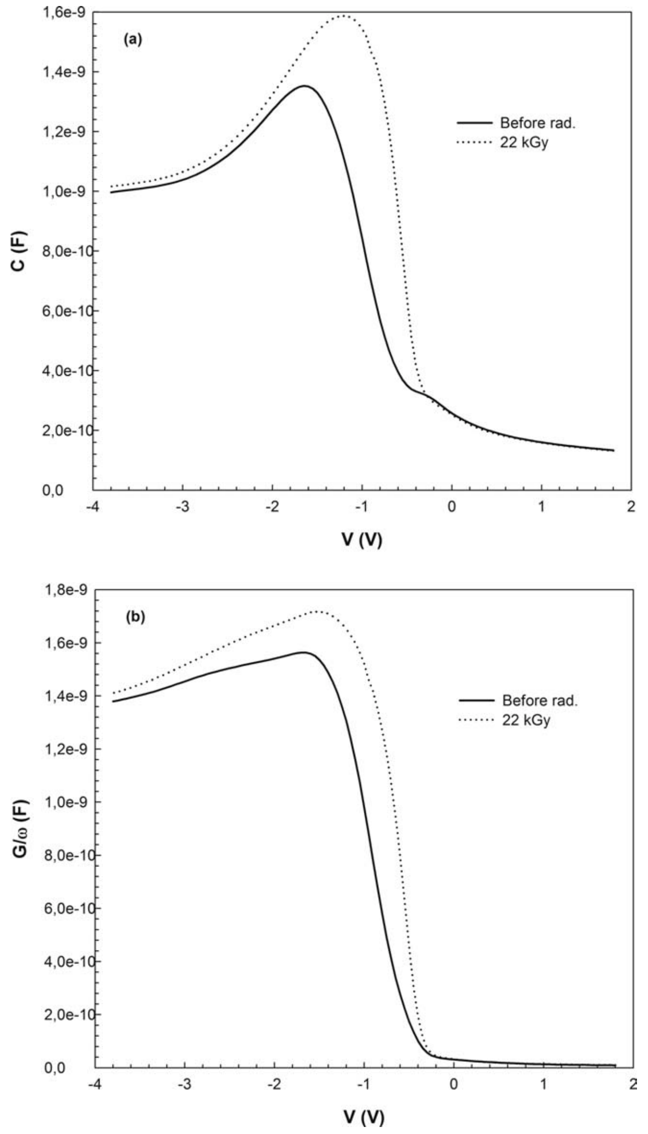

**Figure 5** The measured (a) *C-V* (b) *G/ω-V* characteristics of Au/PVA (Co, Zn-doped)/n-Si Schottky diodes before and after radiation.

$-0{,}35$ V before and after radiation, respectively. It is clearly seen in Figure 6 that the $R_s$ is almost independent of the voltage in both inversion and accumulation regions. We considered that the trap charges have enough energy to escape from the traps located at M/S interface in the Si band gap. The series resistance is an important parameter to designate noise ratio of device as dependent on irradiation dose. The values of $R_s$ obtained from *C-V* and *G/ω-V* measurements decreases with irradiation dose (Fig. 6). The values of $R_s$ become maximum about between $-1\text{V} < V < 0$ V. These peaks shifted to accumulation region with irradiation dose. This behavior of the series resistance can be attributed to particular distribution of interface states.[39] The determined value of $R_s$ changed with applied bias voltage and calculation method.[32,34,39]

To assess some main electrical parameters of Au/PVA (Co, Zn-Doped)/n-Si SBD such as donor concentration $N_D$, fermi energy level $E_F$, the image force lowering of BH $\Delta\Phi_B$, depletion layer width $W_D$, and BH $\Phi_B$ values, the $C^{-2}$ vs. $V$ plots given in Figure 7 were obtained from the *C-V* data before and after irradiation. The relation between $C$ and $V$ for the MS or MIS type SBDs is given as[18,32]

$$C^{-2} = (2/qA^2\varepsilon_s N_D)(V_D - V - kT/q) \tag{13}$$

where $V$ is the applied voltage across the diode and $V_D$ is built-in voltage. $V_D$ is calculated from slope of the linear part of $C^{-2}$ vs. $V$ (Fig. 7) plot at 1MHz before and after irradiation. The $N_D$ value was obtained from the slope of $C^{-2}$ vs. $V$ plot, while the $\Phi_B$ *(C-V)* was obtained from the extrapolated intercept with the $V$-axis ($V_D$-$kT/q$) with aid of following equation as.[18,32]

$$\Phi_B(C-V) = V_0 + \frac{kT}{q} + E_F - \Delta\Phi_B = V_D + E_F - \Delta\Phi_B \tag{14}$$

where $\Delta\Phi_B$ and $E_m$ are the image force barrier lowering and the maximum electric field, respectively, and are given by,[11]

$$\Delta\Phi_B = \sqrt{\frac{qE_m}{4\pi\varepsilon_s\varepsilon_0}} \tag{15a}$$

$$E_m = \sqrt{2qN_D V_D/\varepsilon_s\varepsilon_0} \tag{15b}$$

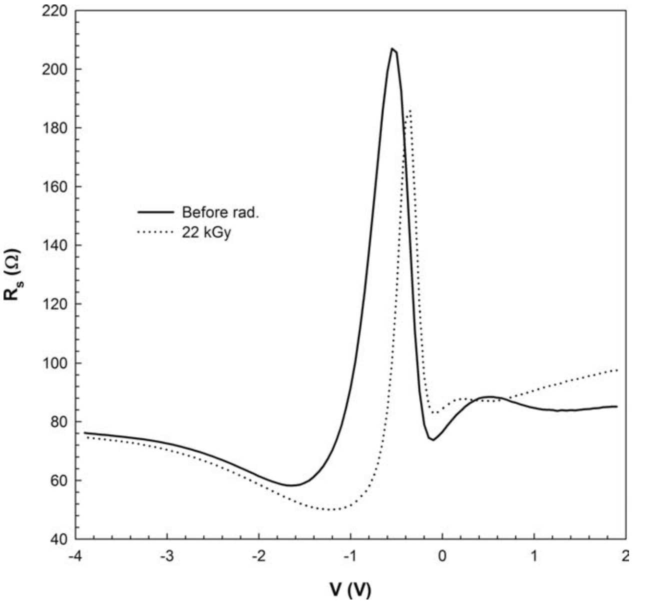

**Figure 6** The $R_s$ characteristics of Au/PVA (Co, Zn-doped)/n-Si Schottky diodes before and after radiation.

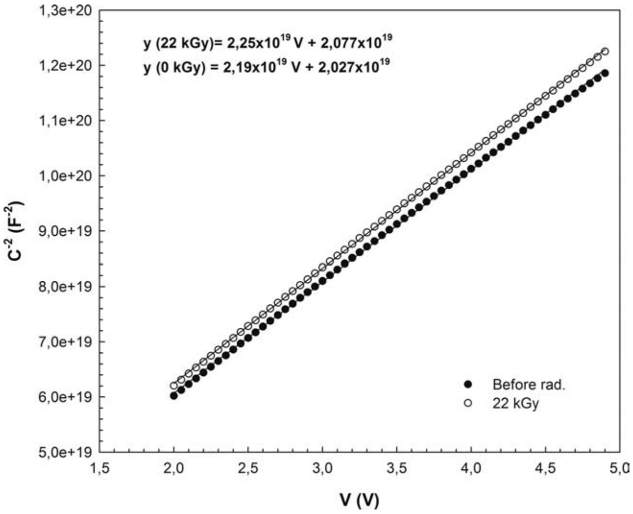

**Figure 7** The $C^{-2}$-$V$ characteristics of Au/PVA (Co, Zn-doped)/n-Si Schottky diodes before and after radiation.

The values of $N_D$ and $\Phi_B$ *(C-V)* for Au/PVA (Co, Zn-Doped)/n-Si SBD were found as $9.58 \times 10^{15}$ cm$^{-3}$ and 1.15 eV before irradiation, and $9.35 \times 10^{15}$ cm$^{-3}$ and 1.148 eV after irradiation, respectively. It is clear that these values were almost unchanged with radiation in the inversion region.

There are several methods have been suggested to determine the $N_{ss}$ profile of MS or MIS type SBDs.[39–43] Among them, the advantage of the high-low frequency capacitance ($C_{HF}$-$C_{LF}$) method comes from the fact that it permits determination of many properties of the interfacial layer, the semiconductor substrate and interface easily. In this method,[42] the $N_{ss}$ can be extracted from its capacitance contribution to the measured experimental *C-V* curve. The equivalent capacitance is the series connection of $C_{ox}$ and surface charge capacitance $C_{sc}$. The values of $N_{ss}$ can be calculated from the measured $C_{unir.}$ and $C_{ir.}$ by using the diode area and $C_{ox}$.[40,42]

$$N_{ss} = \frac{1}{qA}\left[\left(\frac{1}{C_{unir.}} - \frac{1}{C_{ox}}\right)^{-1} - \left(\frac{1}{C_{ir.}} - \frac{1}{C_{ox}}\right)^{-1}\right] \quad (16)$$

The density distribution of $N_{ss}$ profile as function of bias voltage given in Figure 8 was calculated from eq. (16) before (unirradiated) and after irradiation (irradiated). As shown in Figure 8, the values of $N_{ss}$ give a peak at about $-0.85$ V and the maximum value of peak is $9.4 \times 10^{11}$ eV cm$^{-2}$. These values of $N_{ss}$ are corresponding to radiation induced interface states at M/S interface in the Si band gap. Despite the fact that it is seemed a disagreement in the $N_{ss}$ values between their obtained from forward bias *I-V* characteristics (about $10^{12}$–$10^{13}$ eV$^{-1}$ cm$^{-2}$) (Fig. 4) and *C-V* characteristics (about $10^{11}$–$10^{12}$ eV$^{-1}$ cm$^{-2}$) (Fig. 8), when $R_s$ effect is considered, there is a good agreement in $N_{ss}$ with each other. It is concluded that the energy or applied bias voltage dependent values of $N_{ss}$ and the change in $N_{ss}$ is different from region to region.

## CONCLUSIONS

To show the effect of gamma irradiation on the electrical characteristics of Au/PVA (Co, Zn-doped)/n-Si SBD, the forward and reverse bias *I-V*, *C-V*, and *G/w-V* measurements were carried out at room temperature. The values of $n$ and $R_s$ increase with irradiation dose due to an increase of induced by radiation. The degradation in the Au/PVA (Co, Zn-doped)/n-Si SBD properties may be due to the introduction of radiation-induces interfacial defects (between Au and PVA), and lattice defects via displacement damage. The value of $R_s$ increasing with gamma irradiation may be attributed to decrease in the barrier height. The data analyses show that gamma irradiation of diodes increases the reverse saturation current ($I_s$) significantly, while the effect of on the forward current is very small.

In the forward bias, *I-V* characteristics are almost unchanged with radiation. However, in the reverse bias, *I-V* characteristics are dramatically changed after irradiation due to an increase in radiation-induced $N_{ss}$. Therefore, the value of $\Phi_b$ obtained from forward bias *I-V* characteristics is also unchanged with radiation. The energy density of $N_{ss}$ was obtained from the forward bias *I-V* characteristics by taking into account the bias dependence $n$, $\Phi_e$, and $R_s$ of device at room temperature. It shows an exponential growth from midgap of Si toward the bottom of the conductance band before and after irradiation. The value of $N_{ss}$ was also obtained from

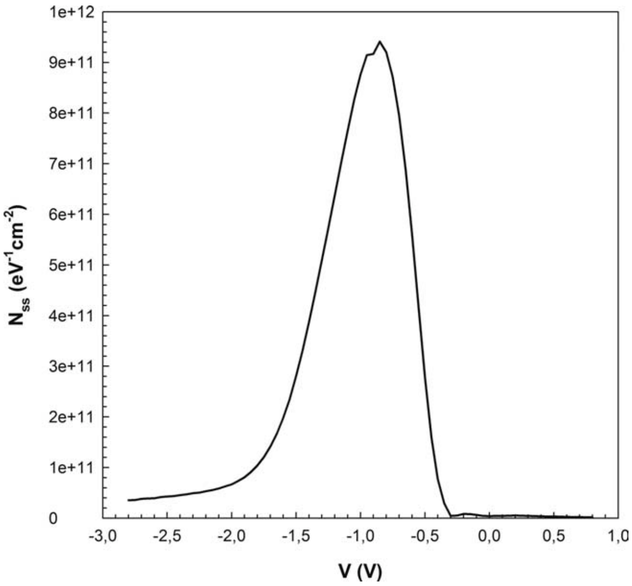

**Figure 8** The $N_{ss}$ profile of Au/PVA (Co, Zn-doped)/n-Si Schottky diodes before and after radiation.

$C_{LF}$-$C_{HF}$ frequency method and the results are almost agreement with each other. In addition, the values of $R_s$ were determined from both Cheung's and admittance methods and the obtained results are good agreement with each other especially for the high bias voltages. In summary, it is clear that the ignoring the effect of $R_s$ and $N_{ss}$ on *I-V*, *C-V*, and *G/ω-V* characteristics can lead to significant errors in the calculations.

## References

1. Connor, B. O.; Pipe, K. P.; Shtein, M. Appl Phys Lett 2008, 92, 193306.
2. Yakuphanoğlu, F. Synth Met 2007, 157, 859.
3. Yakuphanoglu, F.; Okur, S. Microelectron Eng 2010, 87, 30.
4. Aydin, M. E.; Yakuphanoglu, F. Microelectron Eng 2008, 85, 1836.
5. Şahingöz, R.; Kanbur, H.; Voigt, M.; Soykan, C. Synth Met 2008, 158, 727.
6. Farag, A. A. M.; El-Shazly, E. A. A.; Abdel Rafea, M.; Ibrahim, A. Sol Energy Mater Sol Cells 2009, 93, 1853.
7. Dökme, İ.; Altındal, Ş.; Tunç, T.; Uslu, I. Microelectron Reliab 2010, 50, 39.
8. Ozdemir, A. F.; Aldemir, D. A.; Kokce, A.; Altındal, Ş. Synth Met 2009, 159, 1427.
9. Altındal, Ş.; Sari, B.; Unal, H. I.; Yavas, N. J Appl Polym Sci 2009, 113, 2955.
10. Abd El-Kader, F. H.; Attia, G.; Ibrahim, S. S. J Appl Polym Sci 1993, 50, 1281.
11. Ashry, M.; Fayek, S. A. Renewable Energy 2001, 28, 441.
12. Ashok, S.; Borego, J. M.; Gutmann;, R. J. IEEE Trans Nucl Sci 1978, 25, 1473.
13. Karataş, Ş.; Türüt, A.; Altındal, Ş. Radiat Phys Chem 2009, 78, 130.
14. Karataş, Ş.; Türüt, A.; Altındal, Ş. Nucl Instrum Meth Phys Res A 2005, 555, 260.
15. Güllü, Ö.; Türüt, A. J Appl Phys 2009, 106, 103717.
16. Abd El-Kader, F. H.; Attia, G.; Ibrahim, S. S. J Polym Degrad Stab 1994, 43, 253.
17. Sheap, A.; Abd Allah, R. A.; Basha, A. F.; Abd El-Kader, F. H. J Appl Polym Sci 1998, 68, 687.
18. Sze, S. M. Physics of Semiconductor Devices, 2nd ed.; Wiley: New York, 1981.
19. Arslan, E.; Altındal, Ş.; Özçelik, S.; Ozbay, E. J Appl Phys 2009, 105, 023705.
20. Card, H. C.; Rhoderick, E. H. J Phys D: Appl Phys 1971, 4, 1589.
21. Tüzün, O.; Altındal, Ş.; Oktik, Ş. Renewable Energy 2008, 33, 286.
22. Altındal, Ş.; Kanbur, H.; Yücedağ, İ.; Tataroğlu, A. Microelectron Eng 2008, 85, 1495.
23. Chattopadhyay, P.; Raychaudhuri, B. Solid State Electron 1993, 36, 605.
24. Chattopadhyay, P.; Raychaudhuri, B. Solid State Electron 1992, 35, 875.
25. Bülbül, M. M.; Zeyrek, S.; Altındal, Ş.; Yüzer, H. Microelectron Eng 2006, 83, 577.
26. Ho, P. S.; Yang, E. S.; Evans, H. L.; Wu, X. Phys Rev Lett 1986, 56, 177.
27. Hughes, G. W. J Appl Phys 1977, 48, 5357.
28. Umana-Membreno, G. A.; Dell, J. M.; Parish, G.; Nener, B. D.; Faraone, L.; Mishra, U. K. IEEE Trans Electron Dev 2003, 50, 23.
29. Winokur, P. S.; McGarrity, J. M.; Boesch, H. E. IEEE Trans Nucl Sci 1976, 23, 1580.
30. Winokur, P. S.; Schwank, J. R.; Mcwhorter, P. J.; Dressendorfer, P. V.; Turpin, D. C. IEEE Trans Nucl Sci 1984, 31, 1453.
31. Ma, T. P. Semicond Sci Technol 1989, 4, 1061.
32. Rhoderick, E. H.; Williams, R. H. Metal Semiconductor Contacts; Clarendon Press: Oxford, 1988.
33. Uğurel, E.; Aydoğan, Ş.; Şerifoğlu, K.; Türüt, A. Microelectron Eng 2008, 85, 2299.
34. Cheung, S. K.; Cheung, N. W. Appl Phys Lett 1986, 49, 85.
35. Harris, R. D.; Frasca, A. J. IEEE Trans Nucl Sci 2006, 53, **1995.**
36. Pakma, O.; Serin, N.; Serin, T.; Altındal, Ş. Semicond Sci Technol 2008, 23, 105014.
37. Singh, A. Solid State Electron 1985, 28, 223.
38. Altındal, Ş.; Dökme, İ.; Bülbül, M. M.; Yalçın, N.; Serin, T. Microelectron Eng 2006, 83, 499.
39. Nicollian, E. H.; Brews, J. R. MOS Physics and Technology; John Wiley & Sons: New York, 1982.
40. Nicollian, E. H.; Brews, J. R. Bell Syst Tech J 1967, 46, 1055.
41. Çakar, M.; Onganer, Y.; Türüt, A. Synth Met 2002, 126, 213.
42. Castange, R.; Vapaille, A. Surf Sci 1971, 28, 157.
43. Hill, A.; Coleman, C. C. Solid State Electron 1980, 23, 987.